Structure-Function of the G Protein–Coupled Receptor Superfamily

Vsevolod Katritch, Vadim Cherezov, and Raymond C. Stevens

Department of Molecular Biology, The Scripps Research Institute, La Jolla, California 92037; email: stevens@scripps.edu

Annu. Rev. Pharmacol. Toxicol. 2013. 53:531–56

First published online as a Review in Advance on November 8, 2012

The *Annual Review of Pharmacology and Toxicology* is online at pharmtox.annualreviews.org

This article's doi: 10.1146/annurev-pharmtox-032112-135923

Keywords

GPCR structure, ligand recognition, diversity, activation, biased signaling, allosteric modulation, dimerization

Abstract

During the past few years, crystallography of G protein–coupled receptors (GPCRs) has experienced exponential growth, resulting in the determination of the structures of 16 distinct receptors—9 of them in 2012 alone. Including closely related subtype homology models, this coverage amounts to approximately 12% of the human GPCR superfamily. The adrenergic, rhodopsin, and adenosine receptor systems are also described by agonist-bound active-state structures, including a structure of the receptor–G protein complex for the β_2-adrenergic receptor. Biochemical and biophysical techniques, such as nuclear magnetic resonance and hydrogen-deuterium exchange coupled with mass spectrometry, are providing complementary insights into ligand-dependent dynamic equilibrium between different functional states. Additional details revealed by high-resolution structures illustrate the receptors as allosteric machines that are controlled not only by ligands but also by ions, lipids, cholesterol, and water. This wealth of data is helping redefine our knowledge of how GPCRs recognize such a diverse array of ligands and how they transmit signals 30 angstroms across the cell membrane; it also is shedding light on a structural basis of GPCR allosteric modulation and biased signaling.

INTRODUCTION

7TM: seven-transmembrane

A_{2A}AR: A_{2A} adenosine receptor

β_1AR, β_2AR: β_1- and β_2-adrenergic receptors

H_1R: histamine H_1 receptor

D3R: dopamine D3 receptor

M2 and M3: muscarinic acetylcholine receptors M2 and M3

G protein–coupled receptors (GPCRs) comprise the largest protein superfamily in mammalian genomes. They share a common seven-transmembrane (7TM) topology and mediate cellular responses to a variety of extracellular signals ranging from photons and small molecules to peptides and proteins (1). Diversity of the extracellular ligands is reflected in the structural diversity of more than 800 human GPCRs, which can be grouped into five major families and numerous subfamilies on the basis of their amino acid sequences (2). Signal transduction by GPCRs is fundamental for most physiological processes—from vision, smell, and taste to neurological, cardiovascular, endocrine, and reproductive functions—thus making the GPCR superfamily a major target for therapeutic intervention (3, 4). Current drug discovery efforts aim both to improve therapies for more than 50 established GPCR targets and to expand the list of targeted GPCRs (5, 6). In addition to activating GPCR signals with agonists and inhibiting GPCRs with antagonists and inverse agonists, trends in modern pharmacology include discovery of allosteric and/or functionally selective modulators (7) that bias downstream signaling toward specific G protein–activated or β-arrestin-activated pathways (8).

Prior to 2007, GPCR structure and function, which had been extensively probed using biophysical and biochemical methods, was interpreted via ab initio or rhodopsin-based (9) modeling (e.g., reviewed in 10, 11). Breakthrough developments in protein engineering (12, 13) and crystallography (13a–c, 28) galvanized exponential growth in GPCR structure determination (**Figure 1** and **Table 1**). Most of these GPCRs were initially captured in an inactive state stabilized by antagonists or inverse agonists while the elevated conformational plasticity and heterogeneity of the activated states posed additional challenges for crystallization.

The first insights into active-state crystal structures were obtained in 2008 for ligand-free rhodopsin (opsin) (14–16). Selective stabilization of the active conformation resulted in active-state structures of rhodopsin (17, 18, 19), A_{2A} adenosine receptor (A_{2A}AR) (20, 21), and β_2-adrenergic receptor (β_2AR) bound to an agonist, where β_2AR was also stabilized by a heterotrimeric G_s protein (22) or nanobody (23). These crystallographic insights are being greatly complemented by studies of GPCR conformational changes and dynamics that use biochemical methods and spectroscopy.

This review discusses how the recent structural and biophysical insights contribute to our understanding of molecular interactions, subtype, and functional selectivity of ligands, activation mechanisms and conformational dynamics, and other aspects of GPCR biological function. We also outline emerging and future lines of inquiry for studying GPCR signaling mechanisms and harnessing them for drug discovery (24, 25).

STRUCTURAL COVERAGE OF GPCR SUPERFAMILY

Recent Progress in GPCR Structural Characterization

Until 2007, structural information on the highly diverse repertoire of GPCRs (2) was limited to crystal structures of bovine rhodopsin (Class A) and to structures of extracellular domains of the *Secretin* (Class B) (26) and *Glutamate* (Class C) (27) families. By November 2012, structures of 16 different Class A GPCRs had been determined (**Figure 1** and **Table 1**), 9 of them deposited in the year 2012 alone, suggesting an exponential growth trend. Approximately half of the solved structures are aminergic receptors, a cluster of the Class A α-group GPCRs that binds monoamine neurotransmitters and acetylcholine, and that has traditionally played a key role in pharmacology and drug development. These receptors include the β-adrenergic receptors β_2AR (28) and β_1AR (13); the histamine H_1 receptor (H_1R) (29); the dopamine D3 receptor (D3R) (30); and two

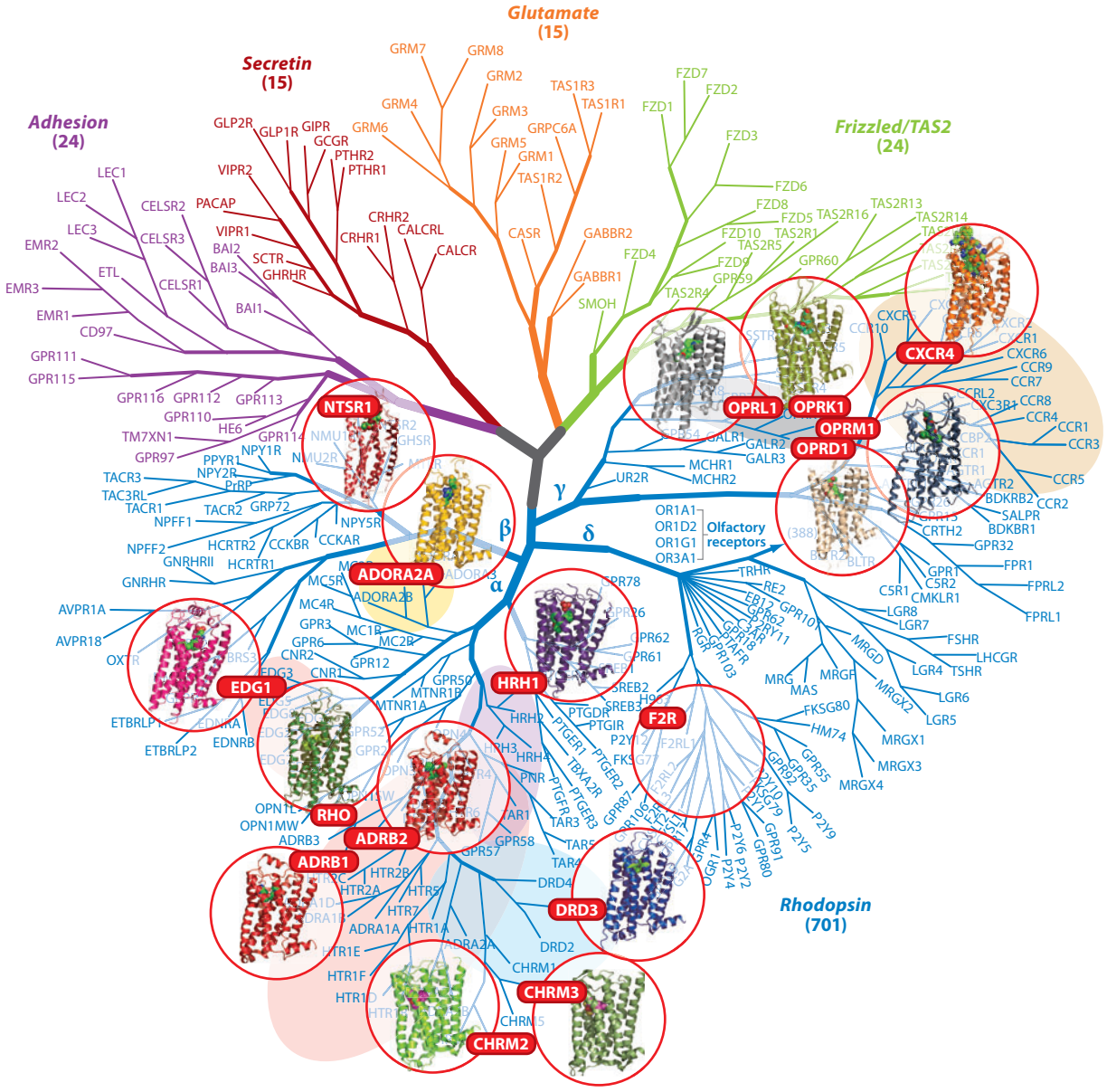

Figure 1

Dendrogram of the human G protein–coupled receptor (GPCR) superfamily with the crystal structures solved by November 2012 [the structure of the protease-activated receptor (F2R) was deposited but had not been released when this review was prepared]. The tree based on sequence similarity in the seven-transmembrane domain is redrawn from Reference 2. According to this notation, human GPCRs include the *Rhodopsin* family (Class A GPCRs), the *Secretin* and *Adhesion* families (Class B GPCRs), the *Glutamate* family (Class C GPCRs), and the *Frizzled/TAS2* family. The *Rhodopsin* family is divided into subgroups: the α-group, the β-group, the γ-group, and the δ-group, as labeled. GPCRs can be further provisionally divided into clusters (e.g., aminergic), subfamilies (e.g., adrenergic or opioid), and individual GPCR subtypes (e.g., dopamine receptor subtypes D1–D5). Olfactory receptors comprise the largest distinct cluster of 388 receptors (only 4 subtypes are shown here) in the δ-group of the *Rhodopsin* family of GPCRs.

Table 1 Crystal structures of GPCRs

Receptor	Gene name	Species	Number of structures	Reference(s)	Year(s)	Resolution (Å)
A_{2A} adenosine	*ADORA2A*	Human	12	20, 21, 46, 47, 79, 116, 117	2008–2012	1.80–3.34
β_1-adrenergic	*ADRB1*	Turkey	12	13, 43, 44, 45	2008–2012	2.30–3.65
β_2-adrenergic	*ADRB2*	Human	11	12, 22, 23, 28, 42, 114, 118	2007–2011	2.40–3.50
Chemokine CXCR4	*CXCR4*	Human	5	34	2010	2.50–3.20
Dopamine D3	*DRD3*	Human	1	30	2010	2.89
Histamine H_1	*HRH1*	Human	1	29	2011	3.10
κ-opioid	*OPRK1*	Human	1	35	2012	2.90
μ-opioid	*OPRM1*	Mouse	1	36	2012	2.90
δ-opioid	*OPRD1*	Mouse	1	37	2012	3.40
Nociceptin/orphanin FQ peptide (NOP)	*OPRL1*	Human	1	38	2012	3.00
Muscarinic M2	*CHRM2*	Human	1	31	2012	3.00
Muscarinic M3	*CHRM3*	Rat	1	32	2012	3.40
$S1P_1$ sphingolipid	*EDG1*	Human	1	33	2012	2.80–3.35
Neurotensin 1	*NTSR1*	Human	1	33a	2012	2.8
PAR1	*F2R*	Rat	1	PDB code 3VW7	2012	2.2
Rhodopsin	*RHO*	Bovine/squid	23/4	9, 40, 15[a]	2000–2012	2.20–4.00

[a]Citations for the rhodopsin structures are shown for the first structure, the highest-resolution structure, and the first active-state structure.

muscarinic acetylcholine receptors, M2 and M3 (31, 32). Other α-group structures include A_{2A}AR (47) and sphingosine-1-phosphate receptor 1 ($S1P_1$) (33) (the first example of a lipid-activated GPCR). Beyond the α-group, the structures of several peptide-binding receptors from the γ-group of Class A GPCRs have been solved, including the chemokine receptor CXCR4 (34), the κ-opioid receptor (κ-OR) (35), the μ-opioid receptor (μ-OR) (36), the δ-opioid receptor (δ-OR) (37), and the nociceptin/orphanin FQ peptide receptor (NOP) (38). Most recently, a structure of the neurotensin receptor 1 representing the Class A β-group was published (33a), and protease-activated receptor 1 from Class A δ-group was deposited [Protein Data Bank (PDB) code 3VW7] but not released at the time of publication.

Opioid receptors are thus far the most comprehensively covered subfamily, with crystal structures of all four closely related opioid subtypes solved, followed by β-adrenergic receptors (two out of three subtypes) and muscarinic acetylcholine receptors (two out of five subtypes). The other solved structures are single representatives of their subfamilies. At the group level of the Class A GPCRs, substantial structural coverage has been achieved for the α-group, for which solved structures of nine GPCRs represent seven distinct subfamilies—approximately half of the subfamilies in the group. At the same time, structural coverage of the γ-group is still sparse, whereas the other two subgroups of the Class A GPCRs (the β- and δ-groups) and the other GPCR classes are just getting their first structural insights.

Several GPCRs, such as rhodopsin (9, 14, 15, 17, 18, 19, 39, 40), β_2AR (22, 23, 28, 41, 42), β_1AR (13, 43, 44, 45), A_{2A}AR (20, 21, 46, 47, 79, 116, 117), and CXCR4 (34), have been cocrystallized in complexes with different ligands, in different crystal forms, or through different approaches to receptor stabilization and crystallization. Importantly, the conformational differences between

$S1P_1$ (or EDG1): sphingosine-1-phosphate receptor 1

CXCR4: chemokine CXCR4 receptor

κ-OR: κ-opioid receptor

μ-OR: μ-opioid receptor

δ-OR: δ-opioid receptor

NOP: nociceptin/orphanin FQ peptide receptor

the multiple inactive-state structures of the same receptor were found to be minor [all-atom root-mean-square deviation (RMSD) < 0.8 angstroms (Å), excluding intracellular loops 2 and 3]; i.e., most key receptor-specific structural features were well preserved. This reproducibility establishes an important baseline for structural comparisons between different GPCRs and between different functional states of these receptors. Modest levels of induced fit in the GPCR binding pockets (42) are also key for effective applications of structures to rational drug discovery. In these applications, hit identification rates as high as 20–70% have been demonstrated in virtual screening for novel antagonist chemotypes in β_2AR (48), A_{2A}AR (49, 50), H_1R (51), D3R (52), and CXCR4 (53), as well as in fragment-based search for derivatives of established agonist scaffolds in adenosine receptors (54).

SI: sequence identity
TM: transmembrane

Structural Diversity Between GPCRs Subfamilies and Subtypes

Although all GPCRs are characterized by a similar 7TM topology, the five major families of human GPCRs (2, 55) (**Figure 1**) share little sequence identity (SI) and possess different extracellular N-terminal domains. [SI < 20% in the transmembrane (TM) domain.] The largest and most diverse *Rhodopsin* family consists of approximately 700 GPCRs in humans, and its subgroups α–δ have an SI of ≥25% (2). Each subgroup contains numerous subfamilies, and GPCR subtypes within these subfamilies share a higher SI (≥30%) and often similar ligand selectivity.

Analysis of structural variations at different levels of homology provides important insights into the scope of structural diversity in GPCRs (reviewed in 56). Within subfamilies, structural similarity between subtypes allows predictions by homology modeling, which can often be accurate enough for many applications. Our initial estimations based on results of blind modeling and docking assessments (57) suggest that homology models based on 35–40% SI can be accurate enough for ligand docking; this was further corroborated by a recent application of such models to virtual screening for D3R antagonists (52) as well as by profiling of ligand selectivity within the adenosine receptor subfamily (58). The 35% SI cutoff for homology modeling yields a rough estimation that the currently solved crystal structures of 16 GPCRs will allow about 12% coverage of the GPCR tree, and at least 100 carefully selected representative receptors will be needed to cover the whole family at this cutoff level.

Importantly, structural variations between different GPCR subfamilies and groups are much more dramatic than within subfamilies. The most striking diversity revealed by crystallography is in the extracellular loop region, which presents a diverse repertoire of secondary structures and disulfide crosslinking patterns (59). Key variations are also found in the 7TM helical bundle itself—including both proline and nonproline kinks and "bulges," π-helices, and other local variations—resulting in deviations as high as ~7 Å in the extracellular tips of TM helices. Most importantly, such variations in extracellular loops, TM helices, and side chains create a remarkable variety of sizes, shapes, and electrostatic properties of the ligand binding pockets in different GPCR subfamilies, reflecting the diversity of their corresponding ligands (**Figure 2**).

With the structure determination of $S1P_1$ (33), the muscarinic acetylcholine receptors (31, 32), and the opioid receptors (35, 36, 37, 38), further examples of structural diversity are added to this repertoire. For example, the structure of a lipid-activated GPCR, $S1P_1$, reveals a unique configuration of the extracellular loop 2 and N terminus, which completely seals the extracellular entrance into the binding pocket. Although rhodopsin also has a tight extracellular "lid" covering the pocket, the backbone structure of these elements in $S1P_1$ is different: Extracellular loop 2 is lacking a secondary structure, a disulfide bond to helix III that is highly conserved in other GPCRs is missing, and the N terminus forms an α-helix on top of the binding pocket. Consistent with the highly lipophilic nature of $S1P_1$ ligands, the structure reveals a "side" opening between

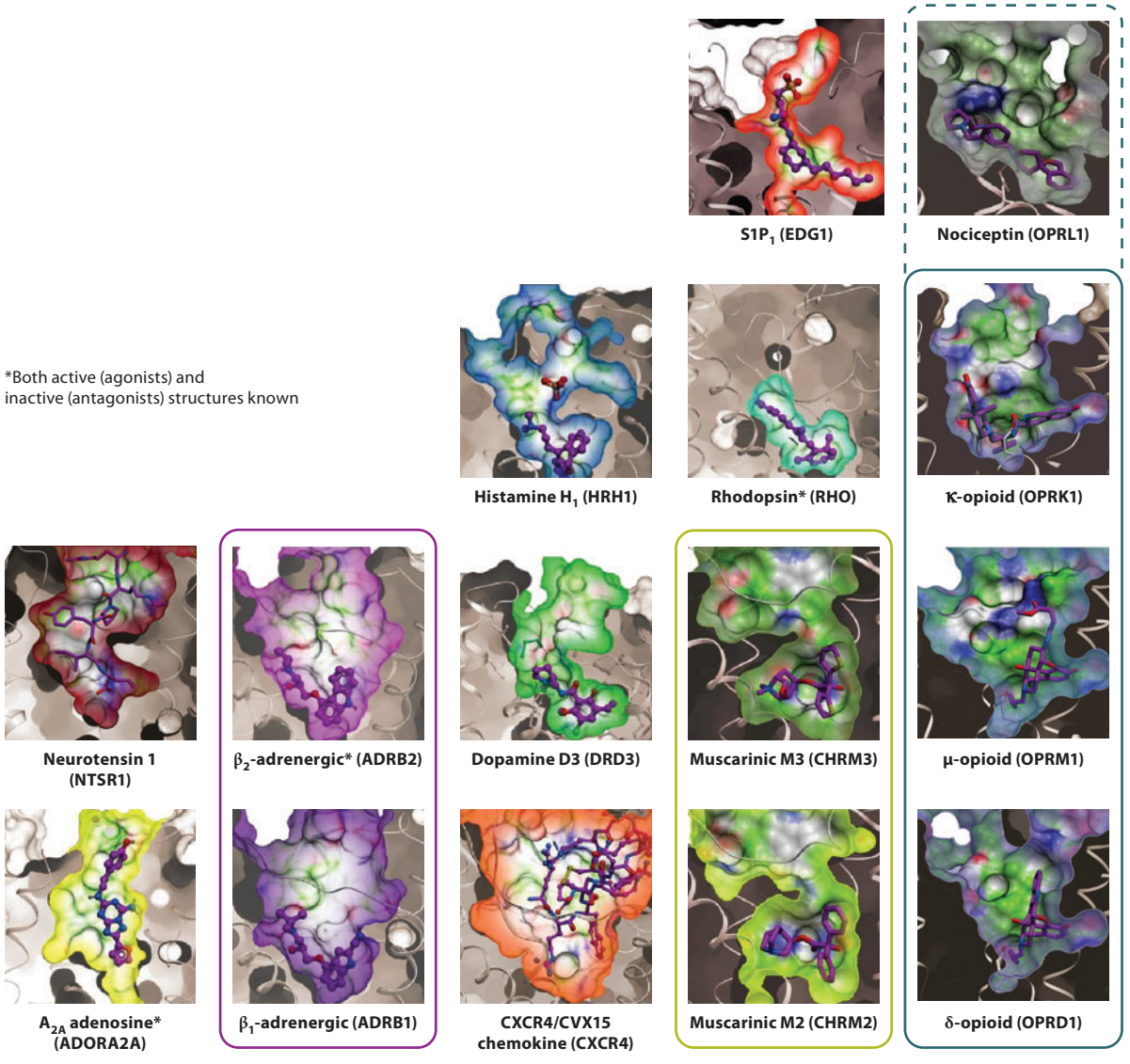

Figure 2

Diversity of ligand binding pockets in G protein–coupled receptors (GPCRs). Pockets are shown as molecular surfaces for available inactive-state GPCR structures in complex with corresponding antagonists. Receptor orientations and the surface clipping planes are the same for all receptors. Pairs of closely related GPCR subtypes with similar pockets are highlighted by colored frames. Abbreviation: $S1P_1$, sphingosine-1-phosphate receptor 1.

Bitopic ligand: chemical compound that targets both ortho- and allosteric sites

helices I and VII that provides direct access of the ligand into the pocket from the lipid bilayer. In contrast, a prominent structural feature of the muscarinic M2 and M3 receptors (31, 32) is a highly restricted entrance to the orthosteric binding pocket controlled by several large aromatic residues. This narrowing creates a separate allosteric pocket in the extracellular loops of the receptor, which potentially plays a role in the ligand-binding kinetics and can accommodate an allosteric modulator or an extended bitopic ligand (32).

Comprehensive Structural Coverage of the Opioid Subfamily

Comprehensive structural coverage of the opioid receptor subfamily (35–38) also provides some unexpected insight into the structural conservation and diversity in GPCRs. Opioid receptor structures exemplify the second subfamily in the peptide-binding γ-group of Class A GPCRs, previously represented only by the chemokine receptor CXCR4 (34). Despite the rather low homology between opioid and chemokine receptors (SI < 27%), these subfamilies have a similar β-hairpin conformation of their extracellular loop 2, which emerges as a common peptide-binding motif in many GPCRs. In contrast, the 7TM bundle region of opioid receptors appears structurally closer to the 7TM region in aminergic receptors from the α-group, with some key common features. For example, all opioid receptors have the same aspartate residue [identified as $Asp^{3.32}$ using Ballesteros-Weinstein numbering (60)], which is also fully conserved in aminergic receptors; in both families, the acidic side chain of $Asp^{3.32}$ serves as a major salt bridge anchor critical for ligand binding and receptor activation.

Ballesteros-Weinstein number: enumeration of GPCR transmembrane residues in X.YY format, where X is the helix number and YY is the residue position relative to the most conserved residue in the helix, designated X.50

Intriguingly, the opioid-like receptor NOP (38), despite high overall SI (60%) with the classical μ-OR (36), κ-OR (35), and δ-OR (37), displays very different ligand selectivity profiles, as it does not bind small-molecule morphine derivatives and binds distinct endogenous peptides. These changes in ligand selectivity are consistent with dramatic structural rearrangements between classical opioid receptors and the NOP, in which replacements of only a few key residues in the ligand binding pocket region result in conformational changes in the backbone structure, including shifts in helices V and VI (38). Such deviations in both ligand selectivity and ligand binding pocket conformations, in spite of the overall high SI, are in stark contrast to the tight conservation of pockets observed in other closely related GPCR subtypes. For example, between β_2AR and β_1AR, as well as between the muscarinic M2 and M3 receptors, the side chains of the core orthosteric binding pockets are identical and have similar conformations. Such divergence of the NOP from classical opioid receptors, accompanied by the switch in ligand selectivity, emphasizes the highly dynamic nature of GPCR evolution in mammalian genomes (61).

STRUCTURAL FRAMEWORK FOR UNDERSTANDING GPCR ACTIVATION

The multitude of biochemical, biophysical, and structural data suggests that most GPCRs exist in a dynamic equilibrium between inactive (R, R′) and active (R″, R*) states, which can be further converted to the signaling state (R^{*G}) in the presence of heterotrimeric G protein, as illustrated in **Figure 3**. Distribution between states in ligand-free receptors can vary drastically, reflecting their different levels of basal activities (62, 63). Inverse agonists shift the equilibrium toward inactive states, decreasing the level of basal activity, whereas neutral antagonists do not affect the basal equilibrium. Binding of agonists shifts the equilibrium toward the activated states, which are characterized by large-scale conformational changes at the receptor's intracellular side (64). Representative examples of these five conformationally distinct functional states have been characterized crystallographically in rhodopsin, A_{2A}AR, and β_2AR (**Table 2**).

Large-Scale Rearrangements of Transmembrane Helices

Remarkably, despite the differences in the identity of receptors, comparisons of inactive- and active-state structures reveal common activation-related features with respect to conformational changes on the intracellular sides of the receptors (**Figure 4*a***). The most pronounced common rearrangement of helices on the intracellular side includes an outward "swinging" motion of helix

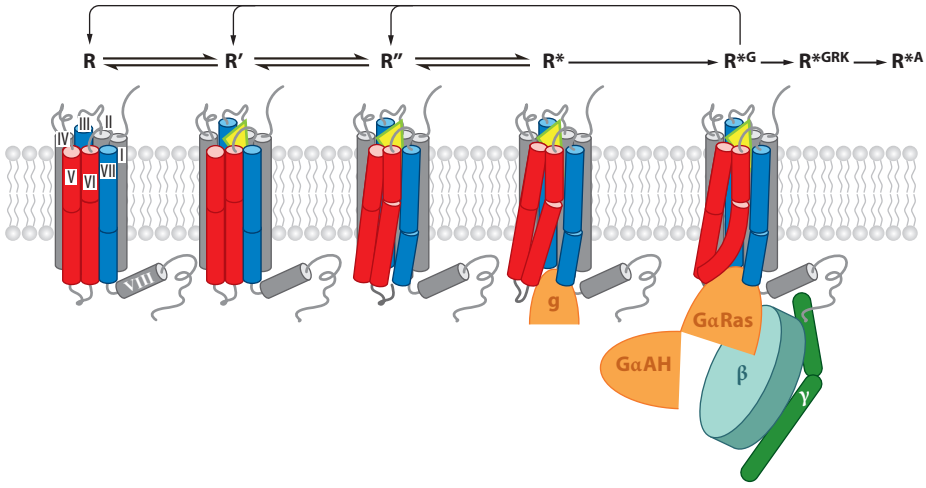

Figure 3

Key intermediates in the G protein–coupled receptor (GPCR) activation mechanism, characterized crystallographically (see **Table 2** for Protein Data Bank codes and references). R represents inactive (ground) states, which can be stabilized by binding of inverse agonists or antagonists. R′ represents inactive low-affinity agonist-bound states, which differ from R states by only small local changes in the receptor binding pocket. R″ represents activated state(s), characterized by substantial global rearrangement of helices and side-chain microswitches on the intracellular side that exposes, at least partially, the G protein binding crevice. R* represents activated substates with initial insertion of the G protein C-terminal α-helix (or its surrogate mimic g) into the intracellular crevice. Finally, R^{*G} is a distinct G protein signaling conformation of a receptor, which can be achieved upon full engagement and activation of the GPCR-Gαβγ complex. Other conformationally distinct states (not depicted) include states for GPCR binding to G protein receptor kinases (R^{*GRK}) and to β-arrestin (R^{*A}). Transition from the initial G protein binding state (R*) to the full signaling state R^{*G} is accompanied by the release of GDP and therefore proceeds unidirectionally; subsequent return to presignaling states requires dissociation of the protein complex and binding of a new Gαβγ-GDP unit to the receptor.

VI in concert with a movement of helix V, as a part of the previously proposed global toggle-switch mechanism (10, 64). The magnitude of this motion varies among different GPCRs and different activated states; for example, the intracellular tip of helix VI moves ∼3.5 Å in A_{2A}AR (R″), ∼6 Å in opsin (R″ and R*), and as much as 11 Å and 14 Å in β_2AR complexes with nanobody (23) and with G protein (R^{*G}) (22), respectively. Moreover, the final positions of the intracellular tips of helices V and VI in the signaling R^{*G} states seem to be controlled largely by dramatic rearrangements in the G protein itself accompanied by GDP release (see **Figure 5*b*** and sidebar, Movements of Transmembrane Helices: Rigid Body or Not?).

Helices III and VII also undergo substantial rearrangements during activation in all three receptors, with the most pronounced changes in this region observed in A_{2A}AR agonist-bound structures (20, 21). The intracellular part of helix VII moves inward toward the middle axis of the 7TM helical bundle and undergoes a marked backbone rearrangement in the region of the conserved NPxxY motif. Motion of helix III consists of an upward shift along its axis and some lateral movement. In β_2AR, the overall shifts of helices III and VII are less pronounced than in A_{2A}AR and rhodopsin, although there is still a substantial distortion in the helix VII NPxxY motif.

These observations suggest that movements of helices V and VI are absolutely essential for G protein binding and activation and are likely conserved in all Class A GPCRs. Movements of helices III and VII more likely depend on the particular receptor and ligand, and although

Table 2 Five distinct activation states represented by crystal structures of GPCRs (PDB codes and corresponding publications shown)

Receptor	R (inactive state)	R′ (inactive agonist-bound state)	R″ (active state)	R* (active state, with Gα mimic)	R^{*G} (G protein signaling state)
A_{2A}AR	3EML (47); 3REY, 3RFM, 3PWH (46); 3VGA, 3VG9 (116); 3UZA, 3UZC (117); 4EIY (79)	n/a	3QAK[a] (20); 2YDO[b], 2YDV[b] (21)	n/a	n/a
β_1AR	2VT4 (13); 2YCW, 2YCX, 2YCY, 2YCZ (43); 4AMI, 4AMJ (45)	2Y00, 2Y01, 2Y02, 2Y03, 2Y04 (44)	n/a	n/a	n/a
β_2AR	2RH1 (12, 28); 2R4R, 2R4S (118); 3D4S (41); 3KJ6 (109); 3NY8, 3NY9, 3NYA (42)	3PDS (114)	n/a	3P0G[c] (23)	3SN6[d] (22)
Rhodopsin	1F88 (9), 1U19 (40)[e]	2G87, 2HPY (39)	3CAP[f] (15)	3DQB[f,g] (14), 2X72[g] (17); 3PQR[g], 3PXO[g] (18); 4A4M[b,g] (19)	n/a

[a]Stabilized by a conformationally selective agonist.
[b]Stabilized in an activated state by point mutations.
[c]Complex with a nanobody mimicking Gα interactions.
[d]Complex with Gαβγ, additionally stabilized by a nanobody.
[e]Out of 15 dark-state rhodopsin structures, only the first and the highest-resolution structures are shown.
[f]Retinal-free opsin.
[g]Complex with C-terminal peptide Gα.
Abbreviations: A_{2A}AR, A_{2A} adenosine receptor; $\beta_{1/2}$AR, $\beta_{1/2}$-adrenergic receptor; GPCR, G protein–coupled receptor; PDB, Protein Data Bank.

their role in G protein activation is not clear yet, they may contribute to G protein–independent signaling pathways (65), as described below.

Conserved Microswitches in GPCR Activation

The global movements of helices during activation are accompanied by a common set of local microswitches in the intracellular parts of GPCRs. The microswitches are characterized by rotamer changes in highly conserved side chains (64) and stabilize the global movements of helices and help prime the intracellular side of a GPCR for G protein binding (**Figure 4*a***).

The D[E]RY sequence in helix III represents one of the most conserved motifs of Class A GPCRs, in which residue $Arg^{3.50}$ (96% conservation among Class A GPCRs) forms a salt bridge to the neighboring acidic side chain $Asp(Glu)^{3.49}$ (Asp 68%, Glu 20%) (66), as found in all inactive-state structures to date. Interestingly, the $Arg^{3.50}$-$Asp^{3.49}$ salt bridge remains intact in the active-state β_2AR-nanobody complex (23), as well as in the activated A_{2A}AR structures (R″) (20, 21). Only in the active-state rhodopsin (R*) and β_2AR (R^{*G}) structures is the salt bridge broken, and the $Arg^{3.50}$ guanidine changes its rotamer conformation to interact with the C-terminal helix of the Gα subunit (14, 17, 18, 22), thus suggesting that the switch in $Arg^{3.50}$ requires the presence of a G protein (**Figure 4*a***).

The $Arg^{3.50}$ side chain can also form an interhelical salt bridge to $Asp^{6.30}$, known as the ionic lock, which connects the intracellular ends of helices III and VI. The ionic lock was first observed

Microswitches: rotamer changes in side chains that are highly conserved between GPCRs

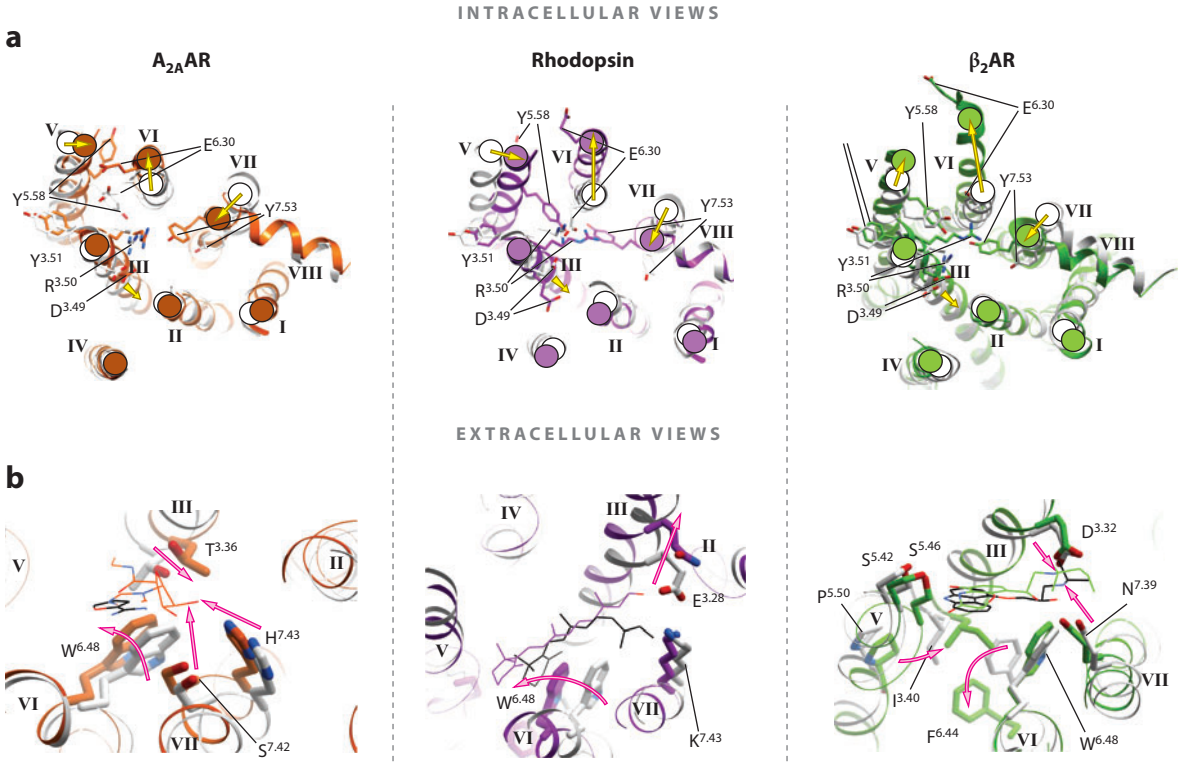

Figure 4

Major conformational rearrangements and ligand-dependent triggers in each of the three available structural models of GPCR activation. (*a*) Intracellular view: common shifts of the intracellular tips of transmembrane helices (*yellow arrows*), which include an outward swinging of helix VI accompanied by a movement of helix V, as well as an inward shift of helix VII and an axial shift of helix III. The established conserved microswitches (*side chains shown as sticks*) undergo rotamer changes upon activation. (*b*) Extracellular view: the key ligand-dependent triggers of GPCR activation (*magenta arrows*) found in the orthosteric site. Trigger residues and their Ballesteros-Weinstein positions are not conserved between these receptors, and the directions of the helical shifts are different. In all panels, inactive conformations are shown in gray, and corresponding activated conformations are shown in color. Ligands are shown by thin lines with black carbons for all antagonists (ZM241385 for $A_{2A}AR$, 11-*cis* retinal for rhodopsin, and carazolol for β_2AR) and with colored carbons for agonists [NECA for $A_{2A}AR$ (*orange*), all-*trans* retinal for rhodopsin (*purple*), and BI-167107 for β_2AR (*green*)]. PDB codes for $A_{2A}AR$: 3EML (47) and 3QAK (20); PDB codes for rhodopsin: 1GZM (119) and 2X72 (17); PDB codes for β_2AR: 2RH1 (28) and 3SN6 (22). Abbreviations: $A_{2A}AR$, A_{2A} adenosine receptor; β_2AR, β_2-adrenergic receptor; GPCR, G protein–coupled receptor; PDB, Protein Data Bank.

in the structures of dark-state bovine rhodopsin, stabilizing this receptor in a fully inactive state (66). The stabilizing role of the ionic lock may be less pronounced in other GPCRs, as it is absent in many GPCR structures, including those with an intact intracellular loop 3 (43), and computer simulations suggest a highly dynamic nature for this interaction (67). Moreover, an acidic residue in position 6.30 is conserved in only ~30% of GPCRs; for example, it is missing in chemokine receptors. Instead, some crystal structures reveal hydrogen-bonding interactions between the $Arg^{3.50}$ side chain and other polar residues in helix VI, such as $Thr^{6.34}$ in κ-OR and μ-OR; these interactions may also play a role in the regulation of receptor signaling.

The NPxxY motif is located near the intracellular end of helix VII and contains a highly (92%) conserved $Tyr^{7.53}$, which serves as a major activation microswitch in GPCRs. In inactive GPCR structures, the side chain of $Tyr^{7.53}$ points toward helix I, II, or VIII. In contrast, in all

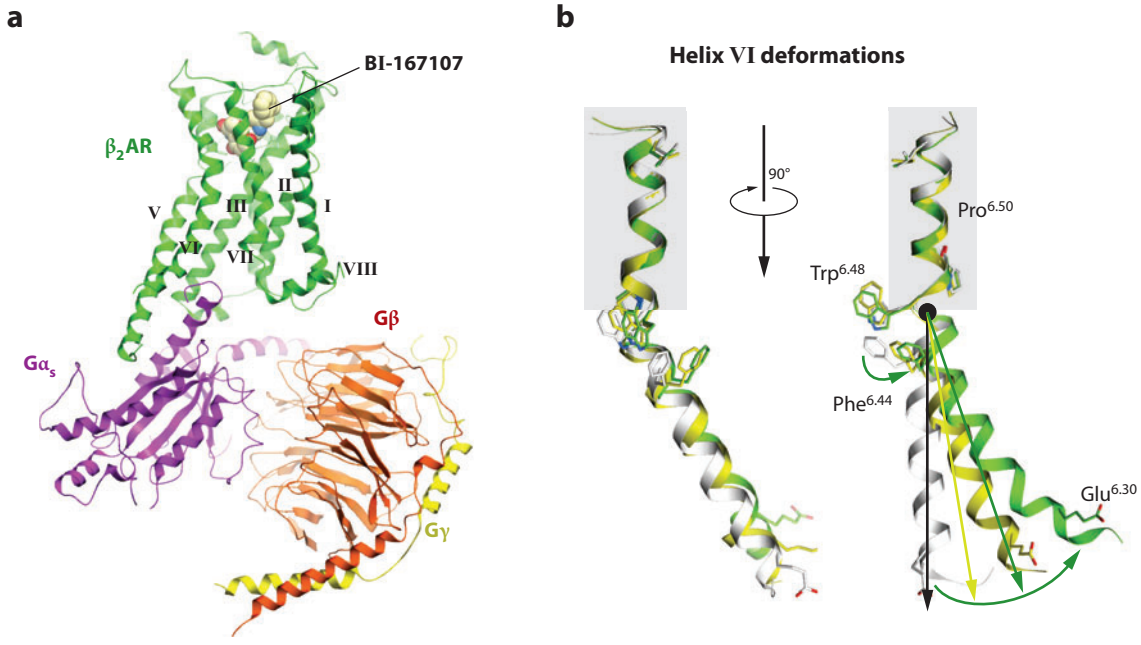

Figure 5

(*a*) Structure of β_2AR in complex with agonist BI-167107 and the G protein heterotrimer (PDB code 3SN6) (22). The receptor and G protein are shown by colored ribbons, whereas the agonist is illustrated by spheres with carbon atoms colored yellow. For clarity, stabilizing nanobody and T4 lysozyme used for crystallization are not shown. (*b*) Conformational changes in helix VI upon β_2AR activation. Structures of inactive R (PDB code 2RH1, *gray*) (28), nanobody-bound R* (PDB code 3P0G, *yellow*) (23), and G protein–bound R^{*G} (PDB code 3SN6, *green*) (22) states are superimposed at the extracellular part of the helix above $Pro288^{6.50}$, highlighted by the gray box. Whereas the bend angle of the $Pro288^{6.50}$-induced kink is maintained, the ligand-stabilized movement of $Phe282^{6.44}$ unwinds the kink, resulting in a swinging motion (combined tilt and rotation) of the intracellular portion of helix VI. Furthermore, the motion of the intracellular part cannot be described entirely in terms of the rigid body but instead shows substantial elastic behavior. This additional bend and displacement of the helix VI tip are apparently induced by insertion of G protein or the nanobody mimic. Abbreviations: β_2AR, β_2-adrenergic receptor; PDB, Protein Data Bank.

active-state GPCR crystal structures, the $Tyr^{7.53}$ side chain changes its rotamer conformation and points toward the middle axis of the 7TM bundle, forming interactions with side chains of helices VI and III. In the active-state structures of β_2AR and rhodopsin, the $Tyr^{7.53}$ hydroxyl may also form a tentative water-mediated hydrogen bond with another putative microswitch, $Tyr^{5.58}$ (89% conserved). Interestingly, the $Tyr^{5.58}$ side chain behaves differently in all three activation models: In rhodopsin, it switches from outside to inside of the helical bundles; in A_{2A}AR, it makes an opposite switch from inside to outside; and in all β_2AR complexes, it remains in the interior of the 7TM bundle. In addition, mutation of $Tyr^{5.58}$ to alanine contributes to the stabilization of β_1AR in its inactive state (68) and to the reduction of basal activity in the muscarinic M3 receptor (69) and thyrotropin receptors (70), although the precise role of this residue in various GPCRs needs further study.

Ligand-Dependent Triggers of GPCR Activation

One of the most intriguing questions of GPCR activation is, How does binding of different ligands in the highly diverse extracellular pockets translate into common large-scale rearrangements on

MOVEMENTS OF TRANSMEMBRANE HELICES: RIGID BODY OR NOT?

The global rearrangements of transmembrane helices during activation are often approximated as rigid body motions (18). Comparison of individual helices in crystal structures of inactive and active GPCRs, however, shows examples of local deformations in helices during activation. One of the most pronounced features is a kink around the highly conserved $Pro^{6.50}$ in helix VI. A superimposition of the extracellular part of helix VI in inactive and activated structures (see the β_2AR example in **Figure 5**) reveals an activation-related "swinging" motion of the intracellular part of helix VI, which involves some unwinding of the helix at the $Pro^{6.50}$ kink. Additional elastic bending of intracellular tip of helix VI in the contact area with G protein or G protein–mimicking nanobody is apparent from the structures, suggesting a force applied in this region by G protein or nanobody insertion. In contrast, in the A_{2A}AR-agonist complex, or in rhodopsin/opsin bound to Gα C-terminal peptide, the intracellular tips of helices V and VI are straight or slightly bent in the direction opposite to that of the overall helical movement (20).

the intracellular sides of different GPCRs? Identification of specific ligand-receptor interactions, or triggers, that control the equilibrium between receptor functional states is critical for understanding and potentially designing efficient agonists, including agonists with desired functional selectivity, also known as bias (71–74). Comparison of multiple active and inactive structures shows modest, but well defined, changes in the binding-pocket residues in each receptor (all-atom RMSD ~1.3 Å for the ligand-contacting residues in β_2AR and A_{2A}AR, and ~2.0 Å for rhodopsin), as illustrated in **Figure 4*b***. These ligand-dependent changes in the binding pockets are also consistent with specific ligand interactions, and their repertoires vary dramatically among the receptors. Some examples of triggers are briefly discussed below; other triggers are likely to be discovered, especially for GPCRs modulated by peptides and/or allosteric ligands.

One of the prominent examples of ligand-dependent rearrangements in the binding pocket involves a shift of the $Trp^{6.48}$ residue, which belongs to the conserved CWxP motif on helix VI. Although this side chain was previously classified as a microswitch (or rotamer toggle switch) (75), crystal structures of active-state GPCRs did not show rotamer changes in this residue upon activation. Moreover, a modified rotamer state of the $Trp^{6.48}$ side chain was observed in inactive muscarinic *M2* and *M3* receptor structures (31, 32), showing that the rotamer state of $Trp^{6.48}$ does not necessarily correlate with the functional state of the receptor. Nevertheless, the crystal structures suggest a prominent role for $Trp^{6.48}$ as a major ligand-dependent trigger in some GPCRs. Thus, A_{2A}AR and rhodopsin active-state structures reveal direct steric interactions of $Trp^{6.48}$ side chains with agonists (20, 21), which stabilize a pronounced shift of $Trp^{6.48}$ and the corresponding swinging movement of helix VI (**Figure 5**). In contrast, the inactive position of $Trp^{6.48}$ can be stabilized by direct interactions with inverse agonists, as observed in rhodopsin–11-*cis*-retinal (9), A_{2A}AR-ZM241385 (47), and histamine H_1–doxepin (29) complexes.

Triggers: direct ligand-receptor interactions that modulate equilibrium between GPCR functional states

Unlike A_{2A}AR and rhodopsin, the β_2AR and β_1AR structures lack any direct contacts between the $Trp^{6.48}$ side chain and agonists or inverse agonists. Instead, conformational changes that promote helix VI motion in β_2AR (23) depend largely on agonists engaging in polar interactions with $Ser203^{5.42}$ and $Ser207^{5.46}$ and stabilizing a ~2-Å inward shift of the extracellular part of helix V, as initially predicted from modeling results obtained with the inactive β_2AR structure (76, 77). Further details of this conformational change, as resolved in the crystal structures of active β_2AR (22, 23), show that this movement in helix V results in a rotamer switching in $Ile121^{3.40}$, which is, in turn, coupled with a 4-Å movement of the $Phe282^{6.44}$ side chain and a corresponding swing of helix VI. Thus, in the case of β_2AR, $Trp^{6.48}$ seems to have only an indirect role in activation, as

also apparent from its <1-Å movement, which is much smaller than in other receptors. Therefore, the role of $Trp^{6.48}$ is not universal, even among the three currently available models of GPCR activation; moreover, approximately 30% of Class A GPCRs have different side chains in the 6.48 position.

Another general site of conformational changes in the binding pocket involves helices III and VII, which are bridged by strong ligand-mediated interactions in all three GPCR activation models. The specifics of the changes in this site, however, vary dramatically for different receptors (**Figure 4*b***). In rhodopsin, light activation results in disruption of a salt bridge between $Glu113^{3.28}$ and the $Lys296^{7.43}$ Schiff base linked to retinal, and it corresponds to an increase of the distance between helices III and VII by approximately 2–3 Å. Conversely, in $A_{2A}AR$, the ribose rings of agonists participate in a strong hydrogen-bonding network with $Thr88^{3.36}$ and $Ser277^{7.42}$/$His278^{7.43}$, decreasing the distance between helices III and VII ~2 Å compared with $A_{2A}AR$ in complex with an inverse agonist. In β_2AR, $Asp113^{3.32}$ and $Asn312^{7.39}$ are bridged by an ethanolamine tail in both agonists and antagonist complexes, and the distance between these residues in β_2AR does not change substantially between the active- and inactive-state crystal structures. Further insights into how engagement of this and other triggers can affect signaling (including biased signaling) can be gained by biophysical methods that are sensitive to receptor dynamics, as discussed below.

G Protein Binding and Signaling

The structure of the β_2AR-G$\alpha\beta\gamma$ signaling complex (22) (**Figure 5*a***) reveals a series of additional conformational changes at the receptor that are controlled largely by the full G$\alpha\beta\gamma$ engagement and activation. As suggested by Rasmussen et al. (22), initial insertion of the $G\alpha_s$ C-terminal α5-helix into the transiently accessible site between β_2AR helices on the intracellular side is likely to resemble insertion of a Gα C-terminal peptide into the rhodopsin structure (14). Engagement of other receptor-G$\alpha\beta\gamma$ interactions leads to a crowbar-like rotation of the $G\alpha_s$ α5-helix by ~30°, remodeling the β6-α5 loop region, followed by a dramatic rotation of the GαAH domain and GDP release (22). All these rearrangements apparently force further displacement of β_2AR helices V and VI, curving helix VI dramatically outward (see **Figure 5*b***), so that its tip is shifted by as much as 14 Å (22) relative to its positions in inactive states.

The β_2AR-G$\alpha\beta\gamma$ crystal structure also reveals the large β_2AR–Gα protein interface formed by intracellular loop 2 and helices V and VI of the receptor, as well as by the α4- and α5-helices, the αN–β1 junction, and the β3-strand of $G\alpha_s$Ras. Notably, the crystallographically resolved parts of the receptor lack direct interactions with the G$\beta\gamma$ subunits. Additional structures of GPCR–G protein complexes may be needed to explain selectivity toward different Gα subtypes, which in some cases may be differentially regulated by biased ligands (74). The structure of the complex also does not reveal any G protein contacts with β_2AR helices VII and VIII, suggesting that activation-related changes in these helices may not be necessary for G protein signaling but possibly may mediate other GPCR interactions, e.g., interactions with β-arrestins.

STRUCTURAL INSIGHTS INTO ALLOSTERISM AND OLIGOMERIZATION

Structural Basis for Allosteric Modulation of GPCRs

GPCR signaling can be affected by a variety of endogenous allosteric modulators in addition to orthosteric ligands, such as regulatory proteins (74a, 74b), lipids and sterols (74c, 78), and

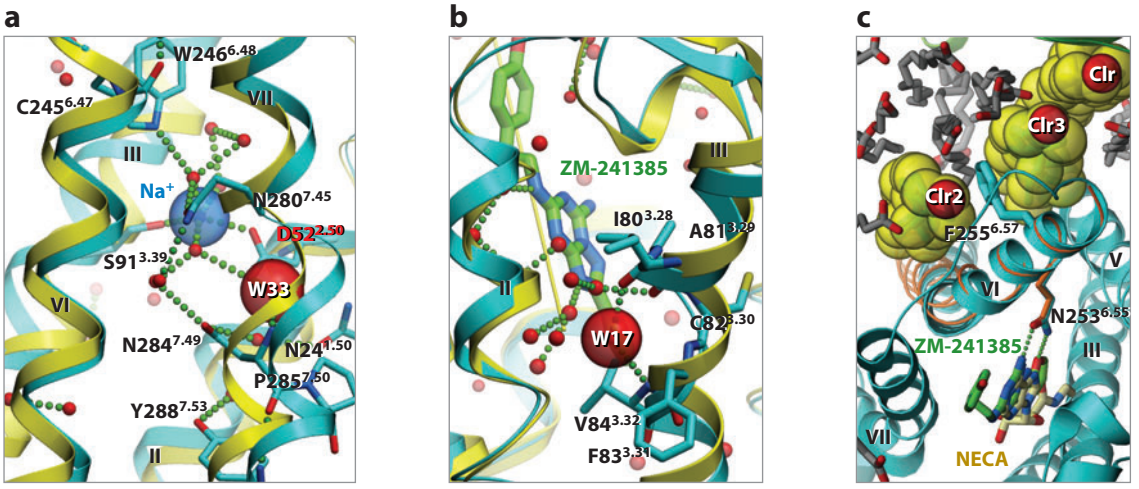

Figure 6

Allosteric sites in the high-resolution inactive $A_{2A}AR$ structure (*blue ribbon and side chains*) (79) compared with the active-state $A_{2A}AR$ complex (*yellow ribbon*) (20). (*a*) Highly conserved in Class A GPCRs is an allosteric site in the middle of the transmembrane bundle. A Na^+/water cluster is observed in the inactive state, but the collapsed pocket in the active state precludes Na^+ binding. (*b*) Tight binding of a structured water in a nonproline kink in helix III of $A_{2A}AR$ is abolished in the active state, where helix III is straightened (*yellow ribbon*). (*c*) Two cholesterol molecules (Clr2 and Clr3) sandwich the phenol ring of Phe255$^{6.57}$ in close proximity of the binding pocket and stabilize the conformation of the extracellular part of helix VI. Abbreviations: $A_{2A}AR$, A_{2A} adenosine receptor; GPCR, G protein–coupled receptor.

ions (71). Moreover, synthetic allosteric and bitopic (7) modulators have been identified for many GPCRs, showing promise as drug candidates with improved subtype selectivity and pharmacological profiles. Several potential allosteric sites in GPCRs revealed by crystal structures have been reviewed (56); these sites include a phosphate ion binding site in the extracellular subpocket of the histamine H_1 structure (29), a cholesterol binding site in β_2AR (41), and a "druggable" extracellular extension of the D3R orthosteric subpocket (30).

New insights into GPCR allosteric regulation come from the 1.8-Å-resolution structure of inactive $A_{2A}AR$ (79), which revealed a tight water-filled channel connecting extracellular and intracellular sides of the receptor. A small (~200-Å^3) allosteric pocket in the middle part of the channel was found to accommodate a Na^+ ion surrounded by a cluster of 10 structured waters (**Figure 6*a***). The pocket is bounded by Trp246$^{6.48}$ (conserved in 71% of Class A GPCRs) on the extracellular side and Tyr288$^{7.53}$ (conserved in 92%) on the intracellular side, as well as residues Asn24$^{1.50}$ (100%), Asp52$^{2.50}$ (94%), Ser91$^{3.39}$ (Ser: 53%, Asp: 26%), Asn280$^{7.45}$ (67%), and Asn284$^{7.49}$ (75%), all of which were predicted to participate in a water-mediated hydrogen-bonding network (64). The negative allosteric modulation effect of Na^+ on agonist binding and activation has been observed in many GPCRs (80) and was tentatively linked to the Asp$^{2.50}$ residue by site-directed mutagenesis (81–83); however, the ion remained undetected in previous medium-resolution structures. The high-resolution $A_{2A}AR$ structure revealed the location of the Na^+ ion coordinated by conserved Asp52$^{2.50}$ and Ser91$^{3.39}$ residues and structured water, rationalizing the stabilizing effect of the Na^+ ion on the inactive receptor state (79). Moreover, analysis of $A_{2A}AR$ crystal structures shows that in the active-state $A_{2A}AR$ (20, 21), the Na^+/water pocket collapses from ~200 to 70 Å^3 due to movements of TM helices. The collapsed pocket does not provide

Allosteric site: receptor binding site distinct from the endogenous ligand (orthosteric) site

adequate coordination for Na^+, suggesting that the ion abandons the pocket and potentially leaves the receptor upon activation (79).

The amino acids in the Na^+/water pocket represent the most conserved spatial cluster of residues in Class A GPCRs (64), suggesting that they share a common role in receptor function. At the same time, any variations in these and surrounding residues that affect the water cluster and Na^+ ion may also alter the dynamics and activation profiles in different GPCRs. Interestingly, whereas the extracellular entrance to the Na^+/water site is somewhat restricted by the $Trp^{6.48}$ side chain in most known GPCR structures, this passage is more open in the muscarinic M2 and M3 receptors (31, 32). A further understanding of the structural and functional details of the pocket will create an opportunity to target this conserved site with allosteric molecules [e.g., amiloride analogs (79)] or bitopic compounds, some of which would have an enhanced ability to stabilize the receptor in the inactive form.

Other potential receptor-specific allosteric sites have also been revealed by recent crystal structures, including a "vestibule" pocket in the extracellular loops of the muscarinic receptors (31, 32), which may bind some of the known allosteric ligands (72, 73). The high-resolution $A_{2A}AR$ structure (79) suggests a cholesterol binding site (**Figure 6*c***) that is distinct from a previously described site in β_2AR (41). Another intriguing observation in this $A_{2A}AR$ structure is a water molecule intercalated at the nonproline kink between residues $Ile80^{3.28}$ and $Val84^{3.32}$, which apparently stabilizes the kinked conformation of helix III (**Figure 6*b***). Importantly, in all agonist-bound active-state structures of $A_{2A}AR$, the kink in this region of helix III is completely straightened, thus precluding water binding. The rearrangement in this water-binding site therefore might play an important role in the activation mechanism of the adenosine receptor subfamily and can be exploited for allosteric modulation through the extension of a ligand scaffold to interact with this site.

GPCR Dimerization and Oligomerization

Although Class A GPCRs can effectively signal as monomers, numerous studies have suggested the existence of homodimers, heterodimers, and higher oligomers in many GPCRs and have proposed their role in the regulation of GPCR function and cross talk (reviewed in 84, 85). GPCR dimerization and oligomerization have been extensively studied using atomic microscopy, fluorescence resonance energy transfer (FRET), bioluminescence resonance energy transfer, cross-linking, time-resolved spectroscopy, and molecular modeling (reviewed in 86, 87), with results systematically collected in the GPCR-OKB database (**http://data.gpcr-okb.org/**) (88). High-resolution structural information on GPCR-GPCR interactions has just started to emerge from crystallographic studies. Parallel dimers with substantial (>600 $Å^2$) protein-protein interfaces have been found in crystal structures of four different GPCRs, including rhodopsin (89), CXCR4 (34), κ-OR (35), and μ-OR (36) (see **Table 3**). Overall, there are two consensus clusters of symmetric interfaces suggested by these structures, which concur with biochemical data for GPCRs such as rhodopsin (90, 91), serotonin 5HT2C (92), dopamine D2 (93, 94), α_{1b}-adrenergic (95, 96), chemotactic C5a (97), and chemokine CCR5 (98). The first cluster of symmetric interfaces, termed interface A (**Figure 7*a***), is found in rhodopsin (15, 89), κ-OR (35), and μ-OR (36) structures. It is formed by helices I, II, and VIII and comprises two separate interaction patches on the extracellular and intracellular sides. Biophysical studies revealed that this dimerization mode is insensitive to receptor activation (92), in agreement with minimal activation-related conformational changes in these interface helices. The second cluster of symmetric interfaces, termed interface B (**Figure 7*b***), involves helices V and VI and, in the case of CXCR4-peptide complexes, can also involve helices III and IV on the intracellular side (34). Similar overall orientation of the dimer subunits, although

Table 3 GPCR transmembrane dimerization interfaces found in crystal structures

Interacting helices	Receptor	Interface (Å^2)	PDB code	Other evidence	Potential implication
Interface A Helices I, II, and VIII	Rhodopsin	~800	2I36, 2I37, 2I35, 3CAP, 4A4M	Cross-linking (90, 91), atomic force microscopy (99)	Functional oligomer
	κ-OR	~1,080	4DJH	Cross-linking in 5HT2C, dopamine D2 (93)	Activation insensitive
	μ-OR	~600	4DKL		
Interface B Helices V, VI (EC); III, IV (IC)	CXCR4	~1,250 850 (EC)+ 400 (IC)	3ODU, 3OE0	Cross-linking in rhodopsin (90, 91), 5HT2C (92), dopamine D2 (94)	Activation sensitive
V, VI bundle	μ-OR	~1,400	4DKL		

Abbreviations: CXCR4, chemokine CXCR4 receptor; EC, extracellular; GPCR, G protein–coupled receptor; IC, intracellular; PDB, Protein Data Bank; κ-OR, κ-opioid receptor; μ-OR, μ-opioid receptor.

with a different contact interface formed by the TM bundles of helices V and VI, has been observed in μ-OR (36). Interface B is likely to hinder receptor activation because its activation requires large conformational movements of helices V and VI. Combined in a repeated pattern, the A and B interfaces are compatible with a high-level oligomerization found in rhodopsin arrays (93, 99), although it is not clear if such a pattern is relevant for the oligomerization observed in other GPCRs (e.g., 95, 96). Further crystallographic, biochemical, and biophysical studies will help elucidate the structural basis and functional role of dimerization interfaces and their variability among different GPCRs.

CONFORMATIONAL DYNAMICS AND SIGNALING BIAS IN GPCRs

As mentioned above, GPCR activation dynamics are characterized by a complex equilibrium among multiple conformational states (100, 101) that is manifested in significant basal activity, the existence of allosteric modulators (73, 102), and a whole spectrum of functional responses including biased signaling (74). A full understanding of these phenomena requires an ability to probe the equilibrium between different conformations, which is beyond the capabilities of crystallographic methods that give a highly detailed but "frozen picture" of the lowest energy receptor state. Various biophysical approaches have shown utility in assessing local and global conformational changes in GPCRs, including fluorescent spectroscopy (100, 103, 104), double electron-electron resonance (105), hydrogen-deuterium exchange coupled with mass spectrometry (106–108), and nuclear magnetic resonance (NMR) spectroscopy (65, 109). Methods are also being developed to assess the kinetics of changes in GPCRs using time-resolved single-molecule studies (110, 111). The availability of 3D structures now allows for the design of optimized labeling sites and provides a structural framework for the analysis of obtained data. Thus, ^{13}C NMR spectroscopy has been employed to assess ligand-dependent conformational changes in the extracellular regions of GPCRs by measuring the formation of a salt bridge that connects extracellular loops 2 and 3 (109) in the β_2AR crystal structure (28). Another NMR technique that has been used to probe dynamics of the intracellular changes in β_2AR exploits spectra of sensitive ^{19}F labels (65). Most notably, the ^{19}F NMR spectra suggested that helices VI and VII can each adopt at least two major

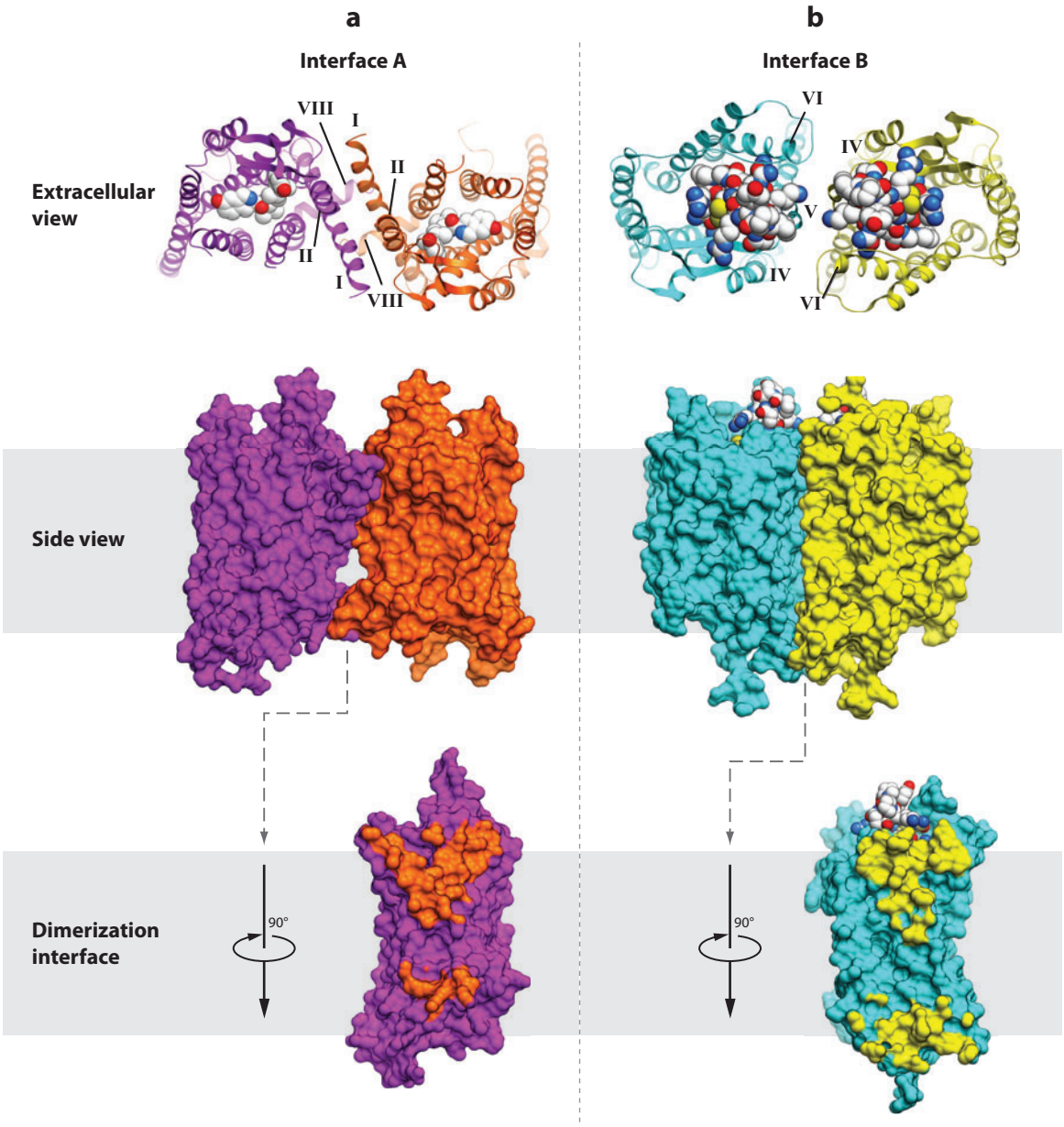

Figure 7

Two clusters of symmetric dimer interfaces observed in GPCR structures: (*a*) interface A and (*b*) interface B. A representative structure of dimer interface A with contacts via helices I, II, VIII is shown for κ-opioid receptor [PDB code 4DJH (35)]. The receptor is shown in orange and magenta, and the JDTic ligand is shown by spheres with white carbons. Interface A has been also observed within μ-opioid receptor, rhodopsin, and opsin structures. A representative structure of interface B involves contacts via helices IV, V, VI (*cyan and yellow*) and is shown here for the CXCR4 complex with peptide antagonist [PDB code 3OE0 (34)]. Similar orientation of subunits has also been observed in the μ-opioid receptor structure [PDB code 4DKL (36)], with an extensive interface formed via helices V and VI. Abbreviations: GPCR, G protein–coupled receptor; PDB, Protein Data Bank.

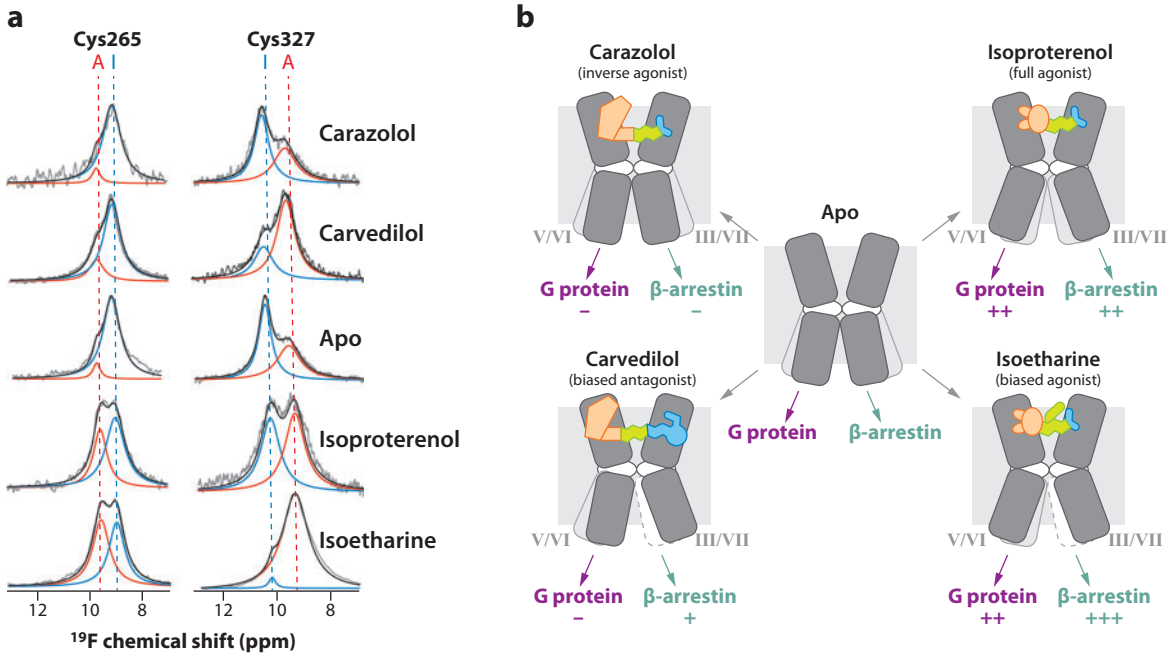

Figure 8

NMR experiments shed light on major signaling pathways in β_2AR (65). (*a*) ^{19}F NMR spectra suggest the existence of at least two distinct states in both Cys265 (helix VI) and Cys327 (helix VII). Equilibrium in each helix is differentially regulated by an agonist (isoproterenol), inverse agonist (carazolol), β-arrestin-biased agonist (isoetharine), and β-arrestin-biased antagonist (carvedilol). (*b*) Suggested differential effects of unbiased (*top row*) and biased (*bottom row*) ligands of G protein–mediated and β-arrestin-mediated signaling. Helices V/VI and III/VII of β_2AR are shown as two sets of bent boxes; the most highly occupied states are shown in dark gray, the less occupied states are shown in light gray, and the minimally occupied states are framed with dotted lines. The arrows underneath each set of boxes indicate the flow of signals associated with changes in specific helices to the corresponding downstream effector. Multiple plus signs (++, +++) indicate higher levels of signaling, and a minus sign (−) indicates reduced signaling, compared with the basal level in unliganded (Apo) receptor. Abbreviations: β_2AR, β_2-adrenergic receptor; NMR, nuclear magnetic resonance.

conformational states that have a slow (>100-ms) exchange rate (**Figure 8**). The equilibrium distribution between these states is controlled by ligand binding: Whereas antagonists and inverse agonists keep β_2AR in a predominantly inactive state, the binding of partial, and especially full, agonists shifts the conformational equilibrium toward an active state in both helix VI and helix VII. The most striking differential effect was observed for the β-arrestin-biased β_2AR ligands carvedilol and isoetharine, both of which showed a dramatic (>40%) increase in the occupancy of the helix VII activated state compared with their unbiased analogs carazolol and isoproterenol, while showing minimal changes in helix VI. These results demonstrate at least a partial decoupling between conformational changes in helices VI and VII, as well as a specific association of helix VII changes with β-arrestin-biased signaling of carvedilol and isoetharine. As described here, association of helix VII with β-arrestin-biased signaling is also supported by recent FRET studies (112), key interactions of β-arrestin with the C-terminal parts of GPCRs adjacent to helix VII (113), and a lack of G protein contacts with helix VII in the β_2AR-G$\alpha\beta\gamma$ signaling complex (22).

Complementary insights into GPCR function can be obtained by molecular modeling approaches, including conformational sampling and flexible ligand-receptor docking (76, 77).

Also, thanks to a rapid growth of computer power and parallelization, unbiased molecular dynamics simulations at a ~10-ms scale has allowed for observations of large conformational changes, i.e., active-to-inactive transitions in β_2AR (114) as well as prediction of ligand-binding paths and kinetics (115). Further structural, biophysical, and computational studies of receptor dynamics, including time-resolved single-molecule studies, will enable researchers to characterize the relationship between various activation states and substates in different GPCRs and to study the possibilities of selectively modulating these states by biased and/or allosteric ligands.

SUMMARY POINTS

1. With the recent breakthroughs in GPCR crystallography, structural coverage of GPCRs has experienced an exponential growth trend, suggesting that receptors from a majority of subfamilies will be solved within the next decade.
2. GPCR structure-function constitutes a challenging research area. The research is best done in a highly collaborative manner, bringing together experts from multiple disciplines to advance the field at the most efficient and rapid rate.
3. Crystal structures of inactive- and active-state GPCRs provide an atomic-level 3D framework for biochemical, biophysical, and computational inquiries into GPCR function and dynamics.
4. All GPCRs have a common 7TM topology; however, they present a great variety of features in their structure, dynamics, selectivity to ligands, modulators, and downstream signaling effectors. Whereas the largest structural variations can be found among different GPCR classes and subfamilies, structures of the opioid receptors reveal substantial structural deviations within the same subfamily, even at 60% sequence identity.
5. Activation mechanisms in GPCRs share several key common features, including movements of helices, side-chain microswitches, and potential rearrangements in the Na^+/water cluster. Conformational changes on the intracellular side are softly coupled to ligand binding through specific ligand-receptor contacts (i.e., triggers). A set of triggers can vary between ligands and between different GPCRs. Preferential engagement of specific triggers by structurally distinct ligands may explain the variety of conformational and functional responses known as biased signaling.
6. Homodimerization, heterodimerization, and oligomerization have been implicated in GPCR regulation and cross talk. Crystallography reveals details of several distinct homodimer interfaces, but additional biochemical and biophysical studies are needed to understand their functional roles in different GPCRs.
7. Crystal structures provide new insights into the allosteric regulation of GPCRs by endogenous ions (e.g. sodium), lipids, cholesterol, and polypeptides, as well as by synthetic molecules, which can modulate GPCR function and pharmacological response. These discoveries highlight the fact that GPCRs are complex allosteric machines that are controlled by more than just their pharmacological ligands.
8. Computer modeling has an important role in creating a comprehensive picture of GPCR structure-function by filling remaining gaps in the superfamily coverage and molecular interactions and by providing a platform for rational drug discovery.

FUTURE ISSUES

1. At least 100 representative GPCRs from subfamilies are proposed to be solved to understand recognition properties. Even more detailed coverage for subfamilies of interest may be helpful for deciphering structural basis of ligand and drug selectivity.
2. In addition to inactive GPCR structures in complex with antagonists, representative structures of active-state agonist-bound complexes are especially critical for full understanding of ligand-specific conformational changes in the binding pocket and details of signal transduction.
3. Availability of crystal structures and purified protein material opens new opportunities to study GPCR dynamics and conformational properties using various biophysical techniques, including nuclear magnetic resonance, hydrogen-deuterium exchange, electron paramagnetic resonance, fluorescent and bioluminescent spectroscopies, and time-resolved single-molecule approaches.
4. We need to employ structural, biophysical, and computational tools to further explore the structural basis of β-arrestin and G protein type selectivity in different receptors in order to gain a better understanding of biased signaling and complex pharmacology of GPCR drugs and drug candidates.
5. The discovery of allosteric control of GPCRs by ions (e.g., sodium), lipids, cholesterol, and water is opening the door to further investigations, expanding our understanding of the functional mechanisms of GPCRs and leading to the discovery of new types of allosteric drug candidates.
6. The issue of receptor oligomerization, and whether receptors use homo- or heterodimerization as part of their function, is once again becoming a debated topic. Complementary in vivo and in vitro studies are needed to clarify this area of receptor structure-function.
7. If we really understand how these receptors work, then we should be able to rationally design ligands to control their function. The application of structural knowledge to successful structure-based drug discovery remains an ultimate goal for the field.

DISCLOSURE STATEMENT

R.C.S. is a founder of Receptos, a GPCR small-molecule drug discovery company, and a founder and member of the board of directors of RuiYi, a GPCR biologics company.

ACKNOWLEDGMENTS

We would like to thank Enrique Abola, Jeff Liu, Irina Kufareva, and Hugo Gutiérrez de Terán for helpful discussions; Katya Kadyshevskaya for help with figure preparation; and Angela Walker for help with manuscript preparation. The work is funded by NIH/NIGMS PSI:Biology grant U54 GM094618.

LITERATURE CITED

1. Lagerstrom MC, Schioth HB. 2008. Structural diversity of G protein-coupled receptors and significance for drug discovery. *Nat. Rev. Drug Discov.* 7:339–57

2. Fredriksson R, Lagerstrom MC, Lundin LG, Schioth HB. 2003. The G-protein-coupled receptors in the human genome form five main families. Phylogenetic analysis, paralogon groups, and fingerprints. *Mol. Pharmacol.* 63:1256–72
3. Overington JP, Al-Lazikani B, Hopkins AL. 2006. How many drug targets are there? *Nat. Rev. Drug Discov.* 5:993–96
4. Tyndall JD, Sandilya R. 2005. GPCR agonists and antagonists in the clinic. *Med. Chem.* 1:405–21
5. Lappano R, Maggiolini M. 2011. G protein-coupled receptors: novel targets for drug discovery in cancer. *Nat. Rev. Drug Discov.* 10:47–60
6. Allen JA, Roth BL. 2011. Strategies to discover unexpected targets for drugs active at G protein–coupled receptors. *Annu. Rev. Pharmacol. Toxicol.* 51:117–44
7. Valant C, Lane JR, Sexton PM, Christopoulos A. 2012. The best of both worlds? Bitopic orthosteric/allosteric ligands of G protein–coupled receptors. *Annu. Rev. Pharmacol. Toxicol.* 52:153–78
8. Reiter E, Ahn S, Shukla AK, Lefkowitz RJ. 2012. Molecular mechanism of β-arrestin-biased agonism at seven-transmembrane receptors. *Annu. Rev. Pharmacol. Toxicol.* 52:179–97
9. Palczewski K, Kumasaka T, Hori T, Behnke CA, Motoshima H, et al. 2000. Crystal structure of rhodopsin: a G protein-coupled receptor. *Science* 289:739–45
10. Schwartz TW, Frimurer TM, Holst B, Rosenkilde MM, Elling CE. 2006. Molecular mechanism of 7TM receptor activation—a global toggle switch model. *Annu. Rev. Pharmacol. Toxicol.* 46:481–519
11. Kobilka BK. 2007. G protein coupled receptor structure and activation. *Biochim. Biophys. Acta* 1768:794–807
12. Rosenbaum DM, Cherezov V, Hanson MA, Rasmussen SG, Thian FS, et al. 2007. GPCR engineering yields high-resolution structural insights into β_2-adrenergic receptor function. *Science* 318:1266–73
13. Warne T, Serrano-Vega MJ, Baker JG, Moukhametzianov R, Edwards PC, et al. 2008. Structure of a β_1-adrenergic G-protein-coupled receptor. *Nature* 454:486–91
13a. Cherezov V, Hanson MA, Griffith MT, Hilgart MC, Sanishvili R, et al. 2009. Rastering strategy for screening and centering of microcrystal samples of human membrane proteins with a sub-10 micron size X-ray synchrotron beam. *J. R. Soc. Interface* 6(Suppl. 5):S587–97
13b. Caffrey M, Cherezov V. 2009. Crystallizing membrane proteins using lipidic mesophases. *Nat. Protoc.* 4:706–31
13c. Cherezov V, Abola E, Stevens RC. 2010. Recent progress in the structure determination of GPCRs, a membrane protein family with high potential as pharmaceutical targets. *Methods Mol. Biol.* 654:141–68
14. Scheerer P, Park JH, Hildebrand PW, Kim YJ, Krauss N, et al. 2008. Crystal structure of opsin in its G-protein-interacting conformation. *Nature* 455:497–502
15. Park JH, Scheerer P, Hofmann KP, Choe HW, Ernst OP. 2008. Crystal structure of the ligand-free G-protein-coupled receptor opsin. *Nature* 454:183–87
16. Park PS, Lodowski DT, Palczewski K. 2008. Activation of G protein–coupled receptors: beyond two-state models and tertiary conformational changes. *Annu. Rev. Pharmacol. Toxicol.* 48:107–41
17. Standfuss J, Edwards PC, D'Antona A, Fransen M, Xie G, et al. 2011. The structural basis of agonist-induced activation in constitutively active rhodopsin. *Nature* 471:656–60
18. Choe HW, Park JH, Kim YJ, Ernst OP. 2011. Transmembrane signaling by GPCRs: insight from rhodopsin and opsin structures. *Neuropharmacology* 60:52–57
19. Deupi X, Edwards P, Singhal A, Nickle B, Oprian D, et al. 2012. Stabilized G protein binding site in the structure of constitutively active metarhodopsin-II. *Proc. Natl. Acad. Sci. USA* 109:119–24
20. Xu F, Wu H, Katritch V, Han GW, Jacobson KA, et al. 2011. Structure of an agonist-bound human A_{2A} adenosine receptor. *Science* 332:322–27
21. Lebon G, Warne T, Edwards PC, Bennett K, Langmead CJ, et al. 2011. Agonist-bound adenosine A_{2A} receptor structures reveal common features of GPCR activation. *Nature* 474:521–25
22. Rasmussen SG, DeVree BT, Zou Y, Kruse AC, Chung KY, et al. 2011. Crystal structure of the β_2 adrenergic receptor–Gs protein complex. *Nature* 477:549–55
23. Rasmussen SG, Choi HJ, Fung JJ, Pardon E, Casarosa P, et al. 2011. Structure of a nanobody-stabilized active state of the β_2 adrenoceptor. *Nature* 469:175–80

24. Reynolds K, Abagyan R, Katritch V. 2010. Structure and modeling of GPCRs: implications for drug discovery. In *GPCR Molecular Pharmacology and Drug Targeting: Shifting Paradigms and New Directions*, ed. A Gilchrist, pp. 385–433. Hoboken, NJ: Wiley
25. Congreve M, Langmead CJ, Mason JS, Marshall FH. 2011. Progress in structure based drug design for G protein-coupled receptors. *J. Med. Chem.* 54:4283–311
26. Archbold JK, Flanagan JU, Watkins HA, Gingell JJ, Hay DL. 2011. Structural insights into RAMP modification of secretin family G protein-coupled receptors: implications for drug development. *Trends Pharmacol. Sci.* 32:591–600
27. Kniazeff J, Prezeau L, Rondard P, Pin JP, Goudet C. 2011. Dimers and beyond: the functional puzzles of class C GPCRs. *Pharmacol. Ther.* 130:9–25
28. Cherezov V, Rosenbaum DM, Hanson MA, Rasmussen SG, Thian FS, et al. 2007. High-resolution crystal structure of an engineered human β_2-adrenergic G protein-coupled receptor. *Science* 318:1258–65
29. Shimamura T, Shiroishi M, Weyand S, Tsujimoto H, Winter G, et al. 2011. Structure of the human histamine H_1 receptor complex with doxepin. *Nature* 475:65–70
30. Chien EY, Liu W, Zhao Q, Katritch V, Han GW, et al. 2010. Structure of the human dopamine D3 receptor in complex with a D2/D3 selective antagonist. *Science* 330:1091–95
31. Haga K, Kruse AC, Asada H, Yurugi-Kobayashi T, Shiroishi M, et al. 2012. Structure of the human M2 muscarinic acetylcholine receptor bound to an antagonist. *Nature* 482:547–51
32. Kruse AC, Hu J, Pan AC, Arlow DH, Rosenbaum DM, et al. 2012. Structure and dynamics of the M3 muscarinic acetylcholine receptor. *Nature* 482:552–56
33. Hanson MA, Roth CB, Jo E, Griffith MT, Scott FL, et al. 2012. Crystal structure of a lipid G protein-coupled receptor. *Science* 335:851–55
33a. White JF, Noinaj N, Shibata Y, Love J, Kloss B, et al. 2012. Structure of the agonist-bound neurotensin receptor. *Nature* 490:508–13
34. Wu B, Chien EY, Mol CD, Fenalti G, Liu W, et al. 2010. Structures of the CXCR4 chemokine GPCR with small-molecule and cyclic peptide antagonists. *Science* 330:1066–71
35. Wu H, Wacker D, Mileni M, Katritch V, Han GW, et al. 2012. Structure of the human κ-opioid receptor in complex with JDTic. *Nature* 485:327–32
36. Manglik A, Kruse AC, Kobilka TS, Thian FS, Mathiesen JM, et al. 2012. Crystal structure of the μ-opioid receptor bound to a morphinan antagonist. *Nature* 485:321–26
37. Granier S, Manglik A, Kruse AC, Kobilka TS, Thian FS, et al. 2012. Structure of the δ-opioid receptor bound to naltrindole. *Nature* 485:400–4
38. Thompson AA, Liu W, Chun E, Katritch V, Wu H, et al. 2012. Structure of the nociceptin/orphanin FQ receptor in complex with a peptide mimetic. *Nature* 485:395–99
39. Nakamichi H, Okada T. 2006. Local peptide movement in the photoreaction intermediate of rhodopsin. *Proc. Natl. Acad. Sci. USA* 103:12729–34
40. Okada T, Sugihara M, Bondar AN, Elstner M, Entel P, Buss V. 2004. The retinal conformation and its environment in rhodopsin in light of a new 2.2 Å crystal structure. *J. Mol. Biol.* 342:571–83
41. Hanson MA, Cherezov V, Griffith MT, Roth CB, Jaakola VP, et al. 2008. A specific cholesterol binding site is established by the 2.8 Å structure of the human β_2-adrenergic receptor. *Structure* 16:897–905
42. Wacker D, Fenalti G, Brown MA, Katritch V, Abagyan R, et al. 2010. Conserved binding mode of human β_2 adrenergic receptor inverse agonists and antagonist revealed by X-ray crystallography. *J. Am. Chem. Soc.* 132:11443–45
43. Moukhametzianov R, Warne T, Edwards PC, Serrano-Vega MJ, Leslie AG, et al. 2011. Two distinct conformations of helix 6 observed in antagonist-bound structures of a β_1-adrenergic receptor. *Proc. Natl. Acad. Sci. USA* 108:8228–32
44. Warne T, Moukhametzianov R, Baker JG, Nehme R, Edwards PC, et al. 2011. The structural basis for agonist and partial agonist action on a β_1-adrenergic receptor. *Nature* 469:241–44
45. Warne T, Edwards PC, Leslie AG, Tate CG. 2012. Crystal structures of a stabilized β_1-adrenoceptor bound to the biased agonists bucindolol and carvedilol. *Structure* 20:841–49
46. Dore AS, Robertson N, Errey JC, Ng I, Hollenstein K, et al. 2011. Structure of the adenosine A_{2A} receptor in complex with ZM241385 and the xanthines XAC and caffeine. *Structure* 19:1283–93

47. Jaakola VP, Griffith MT, Hanson MA, Cherezov V, Chien EY, et al. 2008. The 2.6 angstrom crystal structure of a human A_{2A} adenosine receptor bound to an antagonist. *Science* 322:1211–17
48. Kolb P, Rosenbaum DM, Irwin JJ, Fung JJ, Kobilka BK, Shoichet BK. 2009. Structure-based discovery of β_2-adrenergic receptor ligands. *Proc. Natl. Acad. Sci. USA* 106:6843–48
49. Katritch V, Jaakola VP, Lane JR, Lin J, Ijzerman AP, et al. 2010. Structure-based discovery of novel chemotypes for adenosine A_{2A} receptor antagonists. *J. Med. Chem.* 53:1799–809
50. Carlsson J, Yoo L, Gao ZG, Irwin JJ, Shoichet BK, Jacobson KA. 2010. Structure-based discovery of A_{2A} adenosine receptor ligands. *J. Med. Chem.* 53:3748–55
51. de Graaf C, Kooistra AJ, Vischer HF, Katritch V, Kuijer M, et al. 2011. Crystal structure-based virtual screening for fragment-like ligands of the human histamine H_1 receptor. *J. Med. Chem.* 54:8195–206
52. Carlsson J, Coleman RG, Setola V, Irwin JJ, Fan H, et al. 2011. Ligand discovery from a dopamine D_3 receptor homology model and crystal structure. *Nat. Chem. Biol.* 7:769–78
53. Mysinger MM, Weiss DR, Ziarek JJ, Gravel S, Doak AK, et al. 2012. Structure-based ligand discovery for the protein-protein interface of chemokine receptor CXCR4. *Proc. Natl. Acad. Sci. USA* 109:5517–22
54. Tosh DK, Phan K, Gao ZG, Gakh AA, Xu F, et al. 2012. Optimization of adenosine 5′-carboxamide derivatives as adenosine receptor agonists using structure-based ligand design and fragment-based searching. *J. Med. Chem.* 55:4297–308
55. Fredriksson R, Schioth HB. 2005. The repertoire of G-protein-coupled receptors in fully sequenced genomes. *Mol. Pharmacol.* 67:1414–25
56. Katritch V, Cherezov V, Stevens RC. 2012. Diversity and modularity of G protein-coupled receptor structures. *Trends Pharmacol. Sci.* 33:17–27
57. Kufareva I, Rueda M, Katritch V, Stevens RC, Abagyan R. 2011. Status of GPCR modeling and docking as reflected by community-wide GPCR Dock 2010 assessment. *Structure* 19:1108–26
58. Katritch V, Kufareva I, Abagyan R. 2011. Structure based prediction of subtype-selectivity for adenosine receptor antagonists. *Neuropharmacology* 60:108–15
59. Wheatley M, Wootten D, Conner M, Simms J, Kendrick R, et al. 2011. Lifting the lid on G-protein-coupled receptors: the role of extracellular loops. *Br. J. Pharmacol.* 165:1688–703
60. Ballesteros JA, Weinstein H. 1995. Integrated methods for the construction of three dimensional models and computational probing of structure-function relations in G-protein coupled receptors. *Methods Neurosci.* 25:366–428
61. Strotmann R, Schrock K, Boselt I, Staubert C, Russ A, Schoneberg T. 2011. Evolution of GPCR: change and continuity. *Mol. Cell. Endocrinol.* 331:170–78
62. Seifert R, Wenzel-Seifert K. 2002. Constitutive activity of G-protein-coupled receptors: cause of disease and common property of wild-type receptors. *Naunyn-Schmiedeberg's Arch. Pharmacol.* 366:381–416
63. Kobilka BK, Deupi X. 2007. Conformational complexity of G-protein-coupled receptors. *Trends Pharmacol. Sci.* 28:397–406
64. Nygaard R, Frimurer TM, Holst B, Rosenkilde MM, Schwartz TW. 2009. Ligand binding and micro-switches in 7TM receptor structures. *Trends Pharmacol. Sci.* 30:249–59
65. Liu JJ, Horst R, Katritch V, Stevens RC, Wuthrich K. 2012. Biased signaling pathways in β_2-adrenergic receptor characterized by ^{19}F-NMR. *Science* 335:1106–10
66. Vogel R, Mahalingam M, Ludeke S, Huber T, Siebert F, Sakmar TP. 2008. Functional role of the "ionic lock"—an interhelical hydrogen-bond network in family A heptahelical receptors. *J. Mol. Biol.* 380:648–55
67. Vanni S, Neri M, Tavernelli I, Rothlisberger U. 2009. Observation of "ionic lock" formation in molecular dynamics simulations of wild-type β_1 and β_2 adrenergic receptors. *Biochemistry* 48:4789–97
68. Warne T, Serrano-Vega MJ, Tate CG, Schertler GF. 2009. Development and crystallization of a minimal thermostabilised G protein-coupled receptor. *Protein Expr. Purif.* 65:204–13
69. Li B, Nowak NM, Kim SK, Jacobson KA, Bagheri A, et al. 2005. Random mutagenesis of the M_3 muscarinic acetylcholine receptor expressed in yeast: identification of second-site mutations that restore function to a coupling-deficient mutant M_3 receptor. *J. Biol. Chem.* 280:5664–75
70. Biebermann H, Schöneberg T, Schulz A, Krause G, Grüters A, et al. 1998. A conserved tyrosine residue (Y601) in transmembrane domain 5 of the human thyrotropin receptor serves as a molecular switch to determine G-protein coupling. *FASEB J* 12:1461–71

71. Gao ZG, Jacobson KA. 2006. Keynote review: allosterism in membrane receptors. *Drug Discov. Today* 11:191–202
72. Kenakin T, Miller LJ. 2010. Seven transmembrane receptors as shapeshifting proteins: the impact of allosteric modulation and functional selectivity on new drug discovery. *Pharmacol. Rev.* 62:265–304
73. Keov P, Sexton PM, Christopoulos A. 2011. Allosteric modulation of G protein-coupled receptors: a pharmacological perspective. *Neuropharmacology* 60:24–35
74. Whalen EJ, Rajagopal S, Lefkowitz RJ. 2011. Therapeutic potential of β-arrestin- and G protein-biased agonists. *Trends Mol. Med.* 17:126–39
74a. Thompson MD, Cole DE, Jose PA. 2008. Pharmacogenomics of G protein–coupled receptor signaling: insights from health and disease. *Methods Mol. Biol.* 448:77–107
74b. Ritter SL, Hall RA. 2009. Fine-tuning of GPCR activity by receptor-interacting proteins. *Nat. Rev. Mol. Cell Biol.* 10:819–30
74c. Chini B, Parenti M. 2009. G-protein-coupled receptors, cholesterol and palmitoylation: facts about fats. *J. Mol. Endocrinol.* 42:371–79
75. Shi L, Liapakis G, Xu R, Guarnieri F, Ballesteros JA, Javitch JA. 2002. β_2 adrenergic receptor activation: modulation of the proline kink in transmembrane 6 by a rotamer toggle switch. *J. Biol. Chem.* 277:40989–96
76. Katritch V, Reynolds KA, Cherezov V, Hanson MA, Roth CB, et al. 2009. Analysis of full and partial agonists binding to β_2-adrenergic receptor suggests a role of transmembrane helix V in agonist-specific conformational changes. *J. Mol. Recognit.* 22:307–18
77. Vilar S, Karpiak J, Berk B, Costanzi S. 2011. In silico analysis of the binding of agonists and blockers to the β_2-adrenergic receptor. *J. Mol. Graph. Model.* 29:809–17
78. Escribá PV, Wedegaertner PB, Goñi FM, Vögler O. 2007. Lipid-protein interactions in GPCR-associated signaling. *Biochim. Biophys. Acta* 1768:836–52
79. Liu W, Chun E, Thompson A, Chubukov P, Xu F, et al. 2012. Structural basis for allosteric regulation of GPCRs by sodium ions. *Science* 337:232–36
80. Pert CB, Pasternak G, Snyder SH. 1973. Opiate agonists and antagonists discriminated by receptor binding in brain. *Science* 182:1359–61
81. Jiang Q, Lee BX, Glashofer M, van Rhee AM, Jacobson KA. 1997. Mutagenesis reveals structure-activity parallels between human A_{2A} adenosine receptors and biogenic amine G protein-coupled receptors. *J. Med. Chem.* 40:2588–95
82. Parker MS, Wong YY, Parker SL. 2008. An ion-responsive motif in the second transmembrane segment of rhodopsin-like receptors. *Amino Acids* 35:1–15
83. Selent J, Sanz F, Pastor M, De Fabritiis G. 2010. Induced effects of sodium ions on dopaminergic G-protein coupled receptors. *PLoS Comput. Biol.* 6: e1000884
84. Milligan G. 2009. G protein-coupled receptor hetero-dimerization: contribution to pharmacology and function. *Br. J. Pharmacol.* 158:5–14
85. Maurice P, Kamal M, Jockers R. 2011. Asymmetry of GPCR oligomers supports their functional relevance. *Trends Pharmacol. Sci.* 32:514–20
86. Kaczor AA, Selent J. 2011. Oligomerization of G protein-coupled receptors: biochemical and biophysical methods. *Curr. Med. Chem.* 18:4606–34
87. Selent J, Kaczor AA. 2011. Oligomerization of G protein-coupled receptors: computational methods. *Curr. Med. Chem.* 18:4588–605
88. Khelashvili G, Dorff K, Shan J, Camacho-Artacho M, Skrabanek L, et al. 2010. GPCR-OKB: the G protein coupled receptor oligomer knowledge base. *Bioinformatics* 26:1804–5
89. Salom D, Lodowski DT, Stenkamp RE, Le Trong I, Golczak M, et al. 2006. Crystal structure of a photoactivated deprotonated intermediate of rhodopsin. *Proc. Natl. Acad. Sci. USA* 103:16123–28
90. Taylor MS, Fung HK, Rajgaria R, Filizola M, Weinstein H, Floudas CA. 2008. Mutations affecting the oligomerization interface of G-protein-coupled receptors revealed by a novel de novo protein design framework. *Biophys. J.* 94:2470–81
91. Suda K, Filipek S, Palczewski K, Engel A, Fotiadis D. 2004. The supramolecular structure of the GPCR rhodopsin in solution and native disc membranes. *Mol. Membr. Biol.* 21:435–46

92. Mancia F, Assur Z, Herman AG, Siegel R, Hendrickson WA. 2008. Ligand sensitivity in dimeric associations of the serotonin 5HT2c receptor. *EMBO Rep.* 9:363–69
93. Guo W, Urizar E, Kralikova M, Mobarec JC, Shi L, et al. 2008. Dopamine D2 receptors form higher order oligomers at physiological expression levels. *EMBO J.* 27:2293–304
94. Guo W, Shi L, Filizola M, Weinstein H, Javitch JA. 2005. Crosstalk in G protein-coupled receptors: Changes at the transmembrane homodimer interface determine activation. *Proc. Natl. Acad. Sci. USA* 102:17495–500
95. Lopez-Gimenez JF, Canals M, Pediani JD, Milligan G. 2007. The α_{1b}-adrenoceptor exists as a higher-order oligomer: Effective oligomerization is required for receptor maturation, surface delivery, and function. *Mol. Pharmacol.* 71:1015–29
96. Milligan G, Pediani JD, Canals M, Lopez-Gimenez JF. 2006. Oligomeric structure of the α_{1b}-adrenoceptor: comparisons with rhodopsin. *Vision Res.* 46:4434–41
97. Klco JM, Lassere TB, Baranski TJ. 2003. C5a receptor oligomerization: I. Disulfide trapping reveals oligomers and potential contact surfaces in a G protein-coupled receptor. *J. Biol. Chem.* 278:35345–53
98. Hernanz-Falcon P, Rodriguez-Frade JM, Serrano A, Juan D, del Sol A, et al. 2004. Identification of amino acid residues crucial for chemokine receptor dimerization. *Nat. Immunol.* 5:216–23
99. Fotiadis D, Liang Y, Filipek S, Saperstein DA, Engel A, Palczewski K. 2004. The G protein-coupled receptor rhodopsin in the native membrane. *FEBS Lett.* 564:281–88
100. Yao XJ, Velez Ruiz G, Whorton MR, Rasmussen SG, DeVree BT, et al. 2009. The effect of ligand efficacy on the formation and stability of a GPCR-G protein complex. *Proc. Natl. Acad. Sci. USA* 106:9501–6
101. Deupi X, Kobilka BK. 2010. Energy landscapes as a tool to integrate GPCR structure, dynamics, and function. *Physiology* 25:293–303
102. Goblyos A, Ijzerman AP. 2011. Allosteric modulation of adenosine receptors. *Biochim. Biophys. Acta* 1808:1309–18
103. Gether U, Lin S, Kobilka BK. 1995. Fluorescent labeling of purified β_2 adrenergic receptor: evidence for ligand-specific conformational changes. *J. Biol. Chem.* 270:28268–75
104. Ghanouni P, Gryczynski Z, Steenhuis JJ, Lee TW, Farrens DL, et al. 2001. Functionally different agonists induce distinct conformations in the G protein coupling domain of the β_2 adrenergic receptor. *J. Biol. Chem.* 276:24433–36
105. Altenbach C, Kusnetzow AK, Ernst OP, Hofmann KP, Hubbell WL. 2008. High-resolution distance mapping in rhodopsin reveals the pattern of helix movement due to activation. *Proc. Natl. Acad. Sci. USA* 105:7439–44
106. Lodowski DT, Palczewski K, Miyagi M. 2010. Conformational changes in the G protein-coupled receptor rhodopsin revealed by histidine hydrogen-deuterium exchange. *Biochemistry* 49:9425–27
107. West GM, Chien EY, Katritch V, Gatchalian J, Chalmers MJ, et al. 2011. Ligand-dependent perturbation of the conformational ensemble for the GPCR β_2 adrenergic receptor revealed by HDX. *Structure* 19:1424–32
108. Chung KY, Rasmussen SG, Liu T, Li S, DeVree BT, et al. 2011. Conformational changes in the G protein Gs induced by the $\beta_2$adrenergic receptor. *Nature* 477:611–15
109. Bokoch MP, Zou Y, Rasmussen SG, Liu CW, Nygaard R, et al. 2010. Ligand-specific regulation of the extracellular surface of a G-protein-coupled receptor. *Nature* 463:108–12
110. Kim TY, Uji-i H, Moller M, Muls B, Hofkens J, Alexiev U. 2009. Monitoring the interaction of a single G-protein key binding site with rhodopsin disk membranes upon light activation. *Biochemistry* 48:3801–3
111. Bockenhauer S, Furstenberg A, Yao XJ, Kobilka B, Moerner WE. 2011. Conformational dynamics of single G protein-coupled receptors in solution. *J. Phys. Chem. B* 115:13328–38
112. Rahmeh R, Damian M, Cottet M, Orcel H, Mendre C, et al. 2012. Structural insights into biased G protein-coupled receptor signaling revealed by fluorescence spectroscopy. *Proc. Natl. Acad. Sci. USA* 109:6733–38
113. Nobles KN, Xiao K, Ahn S, Shukla AK, Lam CM, et al. 2011. Distinct phosphorylation sites on the β_2-adrenergic receptor establish a barcode that encodes differential functions of β-arrestin. *Sci. Signal.* 4:ra51
114. Rosenbaum DM, Zhang C, Lyons JA, Holl R, Aragao D, et al. 2011. Structure and function of an irreversible agonist-β_2 adrenoceptor complex. *Nature* 469:236–40

115. Dror RO, Pan AC, Arlow DH, Borhani DW, Maragakis P, et al. 2011. Pathway and mechanism of drug binding to G-protein-coupled receptors. *Proc. Natl. Acad. Sci. USA* 108:13118–23
116. Hino T, Arakawa T, Iwanari H, Yurugi-Kobayashi T, Ikeda-Suno C, et al. 2012. G-protein-coupled receptor inactivation by an allosteric inverse-agonist antibody. *Nature* 482:237–40
117. Congreve M, Andrews SP, Dore AS, Hollenstein K, Hurrell E, et al. 2012. Discovery of 1,2,4-triazine derivatives as adenosine A_{2A} antagonists using structure based drug design. *J. Med. Chem.* 55:1898–903
118. Rasmussen SG, Choi HJ, Rosenbaum DM, Kobilka TS, Thian FS, et al. 2007. Crystal structure of the human β_2 adrenergic G-protein-coupled receptor. *Nature* 450:383–87
119. Li J, Edwards PC, Burghammer M, Villa C, Schertler GF. 2004. Structure of bovine rhodopsin in a trigonal crystal form. *J. Mol. Biol.* 343:1409–38

Annual Review of Pharmacology and Toxicology

Volume 53, 2013

Contents

Indexes

Errata

An online log of corrections to *Annual Review of Pharmacology and Toxicology* articles may be found at http://pharmtox.annualreviews.org/errata.shtml